

Electronic Supplementary Information

Mesoporous Carbon Hollow Spheres: Carbonisation-Temperature-Dependent Delivery of Therapeutic Proteins

Trisha Ghosh,^a Manasi Mantri,^a Zhengying Gu,^a Mohammad Kalantari,^a Meihua Yu^{a,*} and Chengzhong Yu^{a,*}

^aAustralian Institute of Bioengineering and Nanotechnology, The University of Queensland, Brisbane, QLD 4072, Australia,

*Author for correspondence: E-mail: m.yu2@uq.edu.au; E-mail: c.yu@uq.edu.au.

Synthesis of MCHS-*T*

Mesoporous carbon hollow spheres (MCHS) were synthesised according to our previously reported method.¹ Specifically, 12 mM of tetrapropyl orthosilicate (TPOS) was added into an alcoholic solvent system consisting of 70 mL of absolute ethanol and 10 mL of deionized water with 3 mL of ammonium hydroxide (28 wt %) as a catalyst. Then, the above mixture was stirred for 15 minutes at room temperature, followed by simultaneous addition of 0.4 g of resorcinol and 0.56 mL of formalin (37 wt. %). The reaction solution was continuously stirred for 24 hours. The resultant slurry was collected and subjected to high-speed centrifugation at 20,000 rpm for 15 minutes. The solid samples were collected after washing with ethanol for three times and then dried overnight at 50 °C overnight. The hybrid RF polymer/silica samples were carbonised at different temperatures (500, 700, 900 or 1100 °C) for 5 hours under nitrogen environment. The samples were then treated with 10 % hydrogen fluoride (HF, 50 %) solution for at least 24 hours to remove silica templates and washed thoroughly with deionized water for three times. Finally, the carbon samples were obtained after drying at 50 °C overnight and denoted MCHS-*T* (*T*= 500, 700, 900, 1100), where *T* represents the carbonisation temperature in a nitrogen environment.

Flow cytometry analysis to evaluate cellular uptake of MCHS-900 and MCHS-1100

The cellular uptake of MCHS-900 and MCHS-1100 was estimated using flow cytometry analysis. Prior to the cellular study, 5 µg of Rhodamine B Isothiocyanate (RBITC) was completely absorbed in 1 mg of MCHS-900 and MCHS-1100 in 1.5 ml of PBS, washed and resuspended in sterile PBS solution. SCC25 cells were seeded in a 24-well plate with a density of 5×10⁴/well and incubated for 24 hours. Afterwards, 25 µg of RBITC@MCHS-900 or RBITC@MCHS-1100 were added in serum-free DMEM-F12 media. The cells were incubated for 4 hours, and the media was then removed, and the cells were washed with PBS twice. Then the cells were harvested by treating the cells with trypsin, followed by washing with PBS. The cells were suspended in 4 % paraformaldehyde solution for 30 minutes at room temperature, washed again and then resuspended FACS buffer (0.5 % BSA with 5 mM of EDTA in PBS).

Hydrophobicity Test (Rose Bengal Partitioning test)

The hydrophobicity of MCHS-*T* samples was evaluated using a xanthene dye “Rose Bengal” which preferentially gets adsorbed based on the hydrophobicity of the nanoparticles. It is a very reliable method, mainly applied in pharmaceutical studies to determine the surface hydrophobicity of nanoparticle drug delivery systems². At first, in 0.1 M phosphate buffer solution (PBS) with a pH of 7.4, Rose Bengal (RB) reagent was dispersed making an aqueous RB stock solution. The stock solution was diluted to obtain a final concentration of 20 µg/mL. Then the dye solutions were added to various concentrations of nanoparticles (MCHS-*T*), followed by incubation at 25°C for 3 hours. Afterwards, the suspensions were centrifuged at 13,300 rpm for 10 minutes. The supernatants were collected, and absorbance was measured using UV-Vis spectroscopy at 549 nm. Evaluation of hydrophobicity by adsorption of RB was done by determining the PQ (partition quotient). PQ was plotted against the various concentrations of MCHS-*T* to indicate the ratio of an amount of RB [bound] to the MCHS-*T* Vs the RB [free] in the solution, where,

$$RB [bound] = [RB] total concentration - RB [free]$$

Moreover, PQ is calculated as:

$$PQ = RB [bound] / RB [free]$$

The degree of RB entrapment is expressed through the loading capacity and loading efficiency values. Loading capacity (LC) takes the amount of RB entrapped in the particles as a function of the weight of particles. Loading efficiency (LE) is calculated by comparing the amount of RB included in the particles with the total sum of RB. The following equations determined loading capacity (LC) and loading efficiency (LE):

$$LC (\%) = Bound [RB] / weight of particles \times 100$$

$$LE (\%) = bound [RB] / total[RB] \times 100$$

Three batches of particles were prepared in each system, and the results are given as average and standard deviations³.

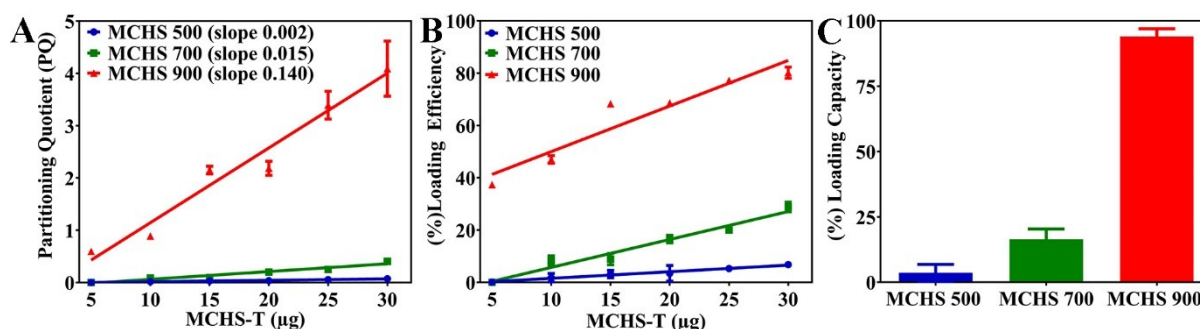


Fig S1. Relative hydrophobicity as measured by adsorption of Rose Bengal on MCHS-*T*. (A) PQ and (B) LE values as a function of the weight of MCHS-*T* and (C) LC of 10 µg of MCHS-*T* towards RB.

PQ values are shown in Fig. S1A showed a higher inclined slope in MCHS-900 (0.140) than MCHS-700 (0.015) and MCHS-500 (0.002), suggestion more adsorption of RB per unit weight. LE values varied from 37 % to 80 % for MCHS-900 when the weight of MCHS-900 increased from 5 to 30 μg (Fig. S1 B). In contrast, the LE value for MCHS-700 ranged from 0% to 30 % while that value for MCHS-500 could only reach maximum 6.9 % of LE given the highest amount of nanoparticles. The evaluation of LC was calculated based on 10 μg of MCHS-*T* in aqueous RB solution. MCHS-500 had the lowest capacity, 3.6 % followed by MCHS-700 with a value of 16.5%. MCHS-900 was proved to have a much higher LC value (94 %) than the other two samples as shown in Fig S1 C. These results consistently indicate that MCHS-900 have the highest hydrophobicity. Higher carbonisation temperature leads to higher hydrophobicity.

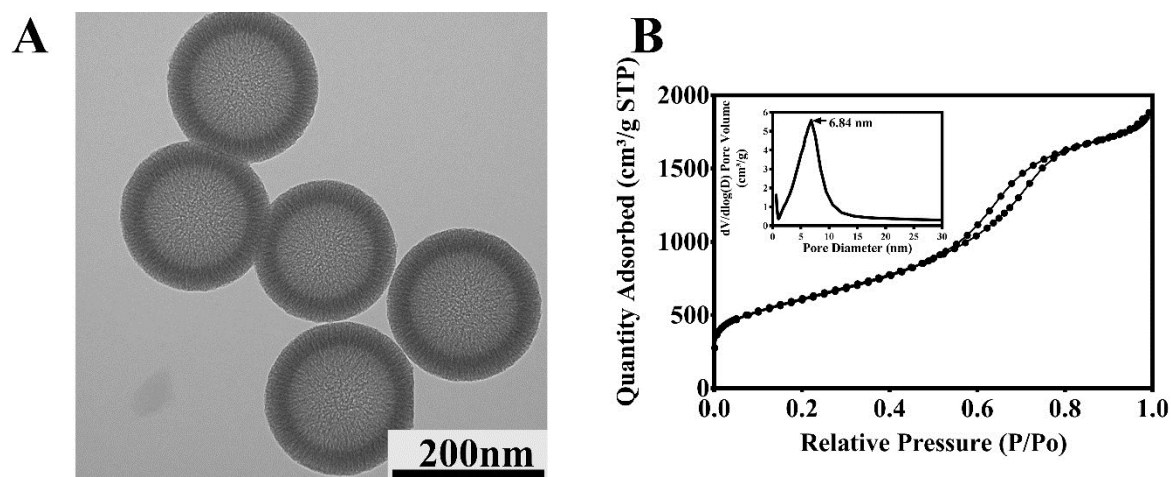


Fig. S2 (A) TEM image and (B) nitrogen adsorption-desorption isotherm and pore size distribution curve (inset) of MCHS-1100.

TEM image of MCHS-1100 (Fig. S2A) reveals a similar intact hollow spherical morphology with mesoporous wall as observed in MCHS-900. The adsorption-desorption plot (Fig. S2B) is typical type IV isotherm with one capillary condensation step at $P/P_0=0.6-0.7$, indicating mesoporous structure. The corresponding pore size distribution curve (inset of Fig. S2B) shows a pore size centred at 6.84 nm, which is similar to MCHS-900. BET surface area and pore volume of MCHS-1100 is 2145.5 m^2/g and 2.9 $\text{cm}^3/\text{g}^{-1}$, respectively.

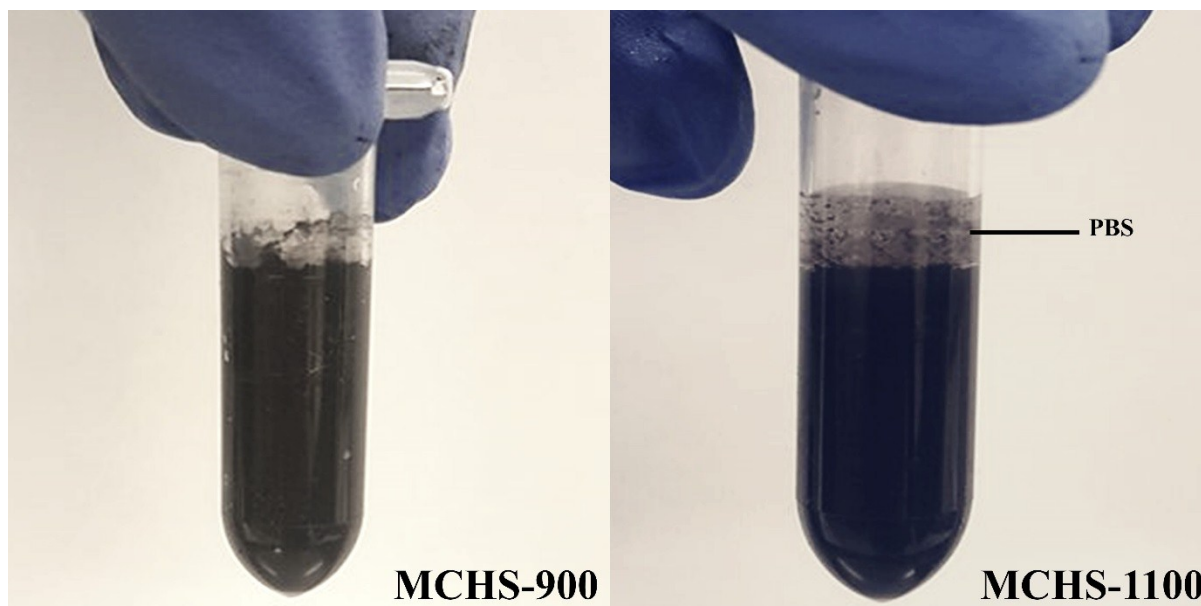


Fig. S3 Images are showing the dispersion of MCHS-900 and MCHS-1100 after ultrasonication. We observed that MCHS-900 had excellent dispersity in PBS buffer solution whereas MCHS-1100 started to separate from the buffer solution and settle as aggregates in PBS after 5 minutes of ultra-sonication.

Additional Discussion: Possible locations of RNase A molecules in MCHS samples

To predict the possible locations of RNase A adsorbed on MCHS samples, RNase A adsorption capacity per unit surface area (mg/m^2) is calculated (as shown in Table S1), dividing loading capacity by BET surface area excluding the unusable micropore area for RNase A adsorption. MCHS-500 has limited porosity, thus RNase A molecules are mainly adsorbed on the external surface, showing a loading capacity of $0.14 \text{ mg}/\text{m}^2$. For MCHS-700 and MCHS-900, the pore size is 6-6.9 nm, which is smaller than double size of 3.8 nm (the largest dimension of single RNase A molecule). Therefore, it is unlikely that the single mesoporous channel on the shell could accommodate two RNase A molecules. In this case, the mesoporous area of MCHS-700 and MCHS-900 is partially used for RNase A adsorption (around 50% or less), thus showing relatively low loading capacity of 0.06 and $0.09 \text{ mg}/\text{m}^2$ for MCHS-700 and MCHS-900. If RNase A molecules are loaded inside the large hollow cavity of MCHS-700 and MCHS-900, these molecules should in a multi-layer adsorption model and the calculated RNase A adsorption capacity per unit surface area would be significantly higher than 0.06 or $0.09 \text{ mg}/\text{m}^2$. Based on these results, we assume that RNase A molecules loaded in MCHS-700 and MCHS-900 are on the surface of carbon materials (mesoporous, external and internal wall) with a mono-layer adsorption model, rather than inside of hollow cores.

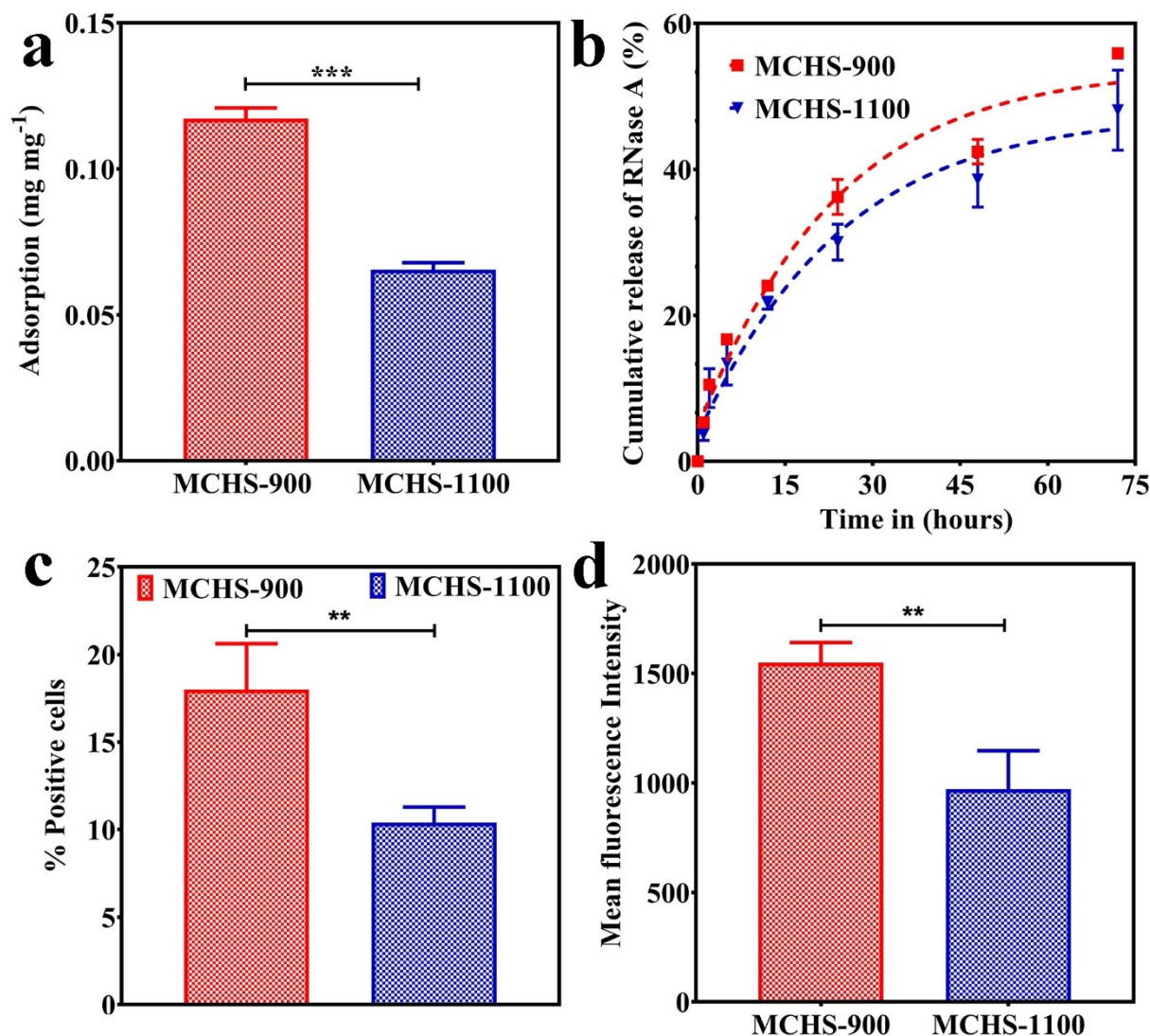


Fig. S4 (a) loading capacity of RNase A, (b) RNase A release profile of MCHS-900 and MCHS-1100, (c) RBITC positive cell percentages and (d) mean fluorescence intensity of SCC25 cells treated with RBITC labelled MCHS-900 and MCHS-1100.

MCHS-1100 shows a much lower RNase A loading capacity than MCHS-900 (0.065 vs 0.117 mg/mg, Fig. S4a) and slightly more sustained release of RNase A (Fig.S4b). To quantify the cellular uptake performance of MCHS-900 and MCHS-1100, flow cytometry was performed in SCC25 cells treated with RBITC loaded carbon samples. The cells treated with RBITC loaded MCHS-900 show significantly larger proportion of RBITC positive cells ($18.0 \pm 2.6\%$ vs $10.4 \pm 0.9\%$, Fig.S4c) and stronger mean fluorescence intensity (1550 ± 91 vs 971 ± 176 , Fig.S4d) than those treated with RBITC loaded MCHS-1100. These results suggest that the low colloidal stability caused by high hydrophobicity significantly impedes the cellular uptake of MCHS-1100, thereby not suitable for cellular delivery of RNase A.

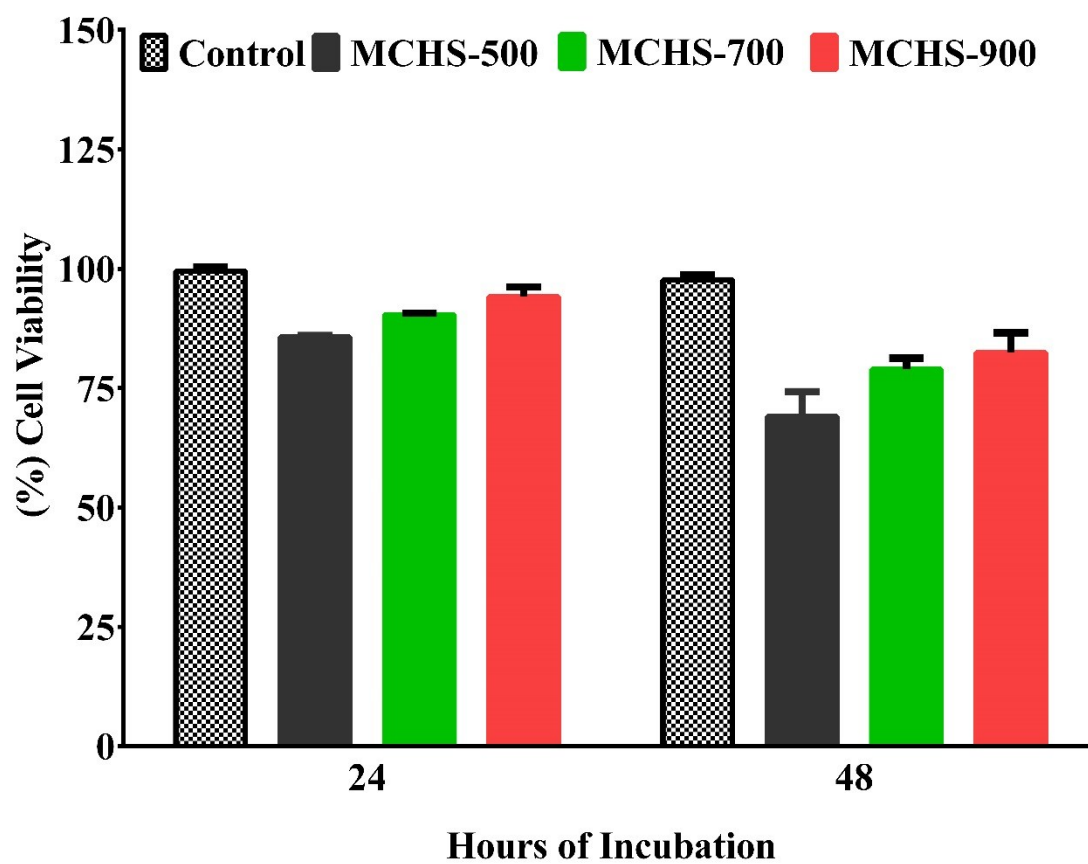


Fig. S5 Cell viability of SCC25 cells treated with bare MCHS-*T* at a high concentration of 200µg/mL to investigate the biocompatibility of the nanocarriers.

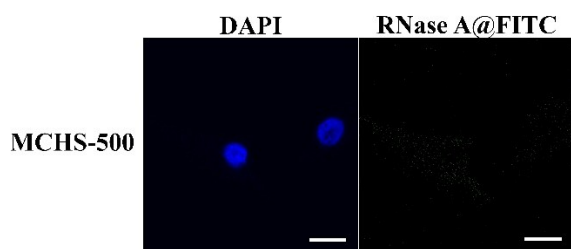


Fig. S6 Confocal Microscopic images of SCC25 showing the fluorescent signals of blue representing DAPI and green representing RNase A tagged with FITC carried inside the cells by MCHS-500, the scale bar is 10 μ m.

Table S1 Calculated RNase A adsorption capacity of MCHS samples.

	MCHS-500	MCHS-700	MCHS-900
S_{BET} ($\text{m}^2 \text{g}^{-1}$)	494	1705	1550
S_{Micro} ($\text{m}^2 \text{g}^{-1}$)	40	231	217
$S_{\text{BET-Micro}}$ ($\text{m}^2 \text{g}^{-1}$)	454	1474	1333
$C_{\text{RNase A}}$ (mg g^{-1})	63.6	89.9	117
$C'_{\text{RNase A}}$ (mg m^{-2})	0.14	0.06	0.09

S_{BET} ($\text{m}^2 \text{g}^{-1}$): BET surface area; S_{Micro} ($\text{m}^2 \text{g}^{-1}$): t-Plot micropore area; $S_{\text{BET-Micro}}$ ($\text{m}^2 \text{g}^{-1}$): BET surface area – t-Plot micropore area; $C_{\text{RNase A}}$ (mg g^{-1}): RNase A adsorption capacity; $C'_{\text{RNase A}}$: RNase A adsorption capacity per m^2 ($C_{\text{RNase A}}/S_{\text{BET-Micro}}$).

References:

1. H. Zhang, O. Noonan, X. Huang, Y. Yang, C. Xu, L. Zhou and C. Yu, *ACS Nano*, 2016, **10**, 4579-4586.
2. Y. Xiao and M. R. Wiesner, *Journal of Hazardous Materials*, 2012, **215**, 146-151.
3. M. C. Moran, A. F. Jorge and M. P. Vinardell, *Biomacromolecules*, 2014, **15**, 3953-3964.